Hindawi
Advances in Civil Engineering
Volume 2023, Article ID 8853122, 20 pages
https://doi.org/10.1155/2023/8853122

Research Article

Low-Code Application and Practical Implications of Common Machine Learning Models for Predicting Punching Shear Strength of Concrete Reinforced Slabs

Khuong Le Nguyen,[1,2] Thanh Tu Do,[1] Giang Huu Nguyen,[1] and Afaq Ahmad[3]

[1]*Department of Civil Engineering, University of Transport Technology, Hanoi 100000, Vietnam*
[2]*Faculty of Arts and Design, University of Canberra, 11 Kirinari Street, Bruce, ACT 2617, Australia*
[3]*Department of Civil Engineering, University of Engineering and Technology, Taxila 47080, Pakistan*

Correspondence should be addressed to Afaq Ahmad; afaq.ahmad@uettaxila.edu.pk

Received 17 May 2023; Revised 25 September 2023; Accepted 10 October 2023; Published 1 November 2023

Academic Editor: Raizal Saifulnaz Muhammad Rashid

This paper investigates the effectiveness of machine learning (ML) models available in MATLAB Regression Learner app and MATLAB App Designer, both low-code applications, for accurately predicting punching shear strength (PSS) in reinforced concrete (RC) slabs. A database of 379 RC slab samples without transverse reinforcement was compiled from renowned publications. RandomSearch and Bayesian optimisation were employed for tuning hyperparameters. The performance of these models was compared with six empirical models, which included three current design codes, three equations from other researchers, and 227 finite-element simulations conducted by the authors. The ML models and finite-element method (FEM) demonstrated superior performance compared with the literature and practical codes. Furthermore, the results emphasised the exceptional performance of the Gaussian process regression (GPR) with optimised hyperparameters, exhibiting the best performance in validation, training, and testing datasets with R^2 values of 0.95, 0.99, and 0.98, respectively. A user-friendly standalone application was developed, providing real-time predictions of the PSS using the two best-developed ML models, GPR and support vector machine (SVM), as well as six empirical models from the literature. This tool offers users flexibility in choosing the most appropriate model for their specific needs, delivering reliable, and accurate results for estimating the PSS of RC slabs.

1. Introduction

In the domain of structural engineering, the accurate prediction of punching shear strength (PSS) in reinforced concrete (RC) slabs is of paramount importance for ensuring the safety, stability, and cost-effectiveness of various building structures. However, when designing such slabs, the brittle punching failure caused by concentrated forces and unbalanced moments between the slabs and columns has severe consequences for the structure [1]. Therefore, estimating PSS is crucial for ensuring the structural safety of these systems.

Recently, alongside traditional approaches like experimental research, analytical models, and finite-element analyses, the machine learning (ML) algorithms have gained popularity for evaluating damage and predicting behaviour in civil, construction, architectural, and structural engineering domains [2–5]. Predicting punching shear resistance in flat slabs has become particularly important in building design. Elshafey et al. [6] employed an artificial neural network (ANN) technique with 244 test data from the literature and experiments to assess the impact of material properties, slab geometry, and boundary conditions. They proposed two new simplified punching shear equations and compared them with models in American, Canadian, British, and European specifications. Chetchotisak et al. [7] and Tran and Kim [8] created ANN-based models for estimating the PSS of reinforced concrete slabs without shear reinforcement, using 342 and 218 experimental tests, respectively. Nguyen et al. [9] developed a ML model utilising XGBoost for 497 experimental data points of interior slab columns and compared the results with two other ML models incorporating ANNs and

random forests (RFs). This concise overview indicates that ANNs have been predominantly employed for predicting PSS in flat slabs without transverse reinforcement, with growing evidence of the efficacy of other ML models such as SVR [10].

This research represents a pioneering effort to explore the use of Gaussian process regression (GPR), support vector machine (SVM), and ensemble ML algorithms for predicting the PSS of RC slabs. The study employs low-code tools like the MATLAB Regression Learner app, which have not been investigated in previous research. In particular, the GPR, a nonparametric and probabilistic model, was thoroughly examined. It offers several advantages over alternative ML techniques, such as providing confidence intervals for predictions, adapting to diverse datasets, and being suitable for small data samples [11].

This study's critical aspect is optimising GPR hyperparameters using random search and Bayesian Optimisation processes, both integrated within the Regression Learner app. Hyperparameter optimisation is essential for enhancing ML model performance [12, 13], and these two techniques have demonstrated effectiveness in identifying optimal hyperparameters across various applications [14, 15]. By incorporating GPR with optimised hyperparameters, the objective is to develop a robust and accurate model that surpasses conventional methods in performance.

Furthermore, this study aims to develop and compare finite-element method (FEM) simulations with ML models for predicting PSS. FEM, a widely used computational technique in structural engineering, has long been employed for analysing complex physical phenomena [16–19]. By contrasting these computational approaches, this research intends to offer valuable insights into the advantages and disadvantages of each method and identify the most suitable technique for practical applications.

To support these computational methods, a user-friendly web application has been developed, which incorporates various practical codes and ML models for quickly predicting the PSS of RC slabs. This application serves as a valuable resource for engineers and designers, streamlining the process of estimating PSS and enhancing overall efficiency.

2. Methodology

The research methodology is outlined in Figure 1. Initially, a database consisting of 379 samples was compiled. The entire dataset was divided into a training set (80% of the data) and a test set (20% of the data). The training set was employed to train and fine-tune the predictive models, while the test set was utilised for evaluating the models' performance. Four common ML algorithms available in the MATLAB Regression Learner app were implemented. Ten models with varying default levels of hyperparameters were initially assessed for model selection.

A tenfold cross-validation procedure was employed to minimise the variance of the findings and provide a more accurate representation of the models' overall performance. Specifically, the training dataset was divided into ten subsets or "folds," and each fold was trained and tested independently. The average of the ten evaluations was used to determine the models' overall performance.

Random search and Bayesian optimisation processes with Gaussian Process surrogate models were applied to optimise the hyperparameters of the four ML models across 500 iterations. The performance of the optimised models was compared with that of the initial models. The best-performing model was evaluated against current design codes, empirical equations, and the FEM.

The performance of the optimised models was further investigated through Monte Carlo simulations, with 600 simulations conducted. Finally, a user-friendly web-based application was developed for estimating the PSS of flat concrete slabs.

2.1. Utilising MATLAB Regression Learner App and MATLAB App Designer. In this research, two modules of MATLAB that utilise low-code development are employed. These applications are designed to facilitate the development process of ML models and to create a user-friendly tool for predicting the PSS—a measure of a concrete structure section's capacity to withstand a punching load.

The MATLAB Regression Learner app, a graphical user interface (GUI) of MATLAB's Statistics and machine learning toolbox, provides a platform for training, testing, and comparing ML regression models. This app streamlines the process of selecting, training, and evaluating regression models by automating many routine tasks, allowing users to focus more on modelling and less on coding. It includes various regression algorithms, like linear regression and decision trees, among others, as well as data preprocessing tools for feature scaling, outlier detection, and missing value imputation. The MATLAB Regression Learner app is noted for its ease of use, automated model selection and optimisation, performance evaluation metrics, data preprocessing tools, and seamless integration with MATLAB itself. The results derived from this research are illustrated in Figure 2.

MATLAB's App Designer is another low-code application that streamlines the creation of interactive, user-friendly applications with scustomised interfaces. This robust tool simplifies the design and implementation of graphical interfaces for a variety of applications, enabling users to develop visually pleasing and straightforward apps that incorporate advanced computational tools.

In this research, App Designer is employed to craft a standalone application that integrates the ML models developed using the Regression Learner app. The ensuing application offers an intuitive interface, enabling users to input pertinent data and secure accurate predictions of the PSS of RC slabs. As such, it bridges the gap between advanced computational methodologies and practical engineering applications.

The utilisation of MATLAB's App Designer in this context highlights the significance of low-code platforms in improving the accessibility and usability of sophisticated tools and models in the realm of civil engineering. The

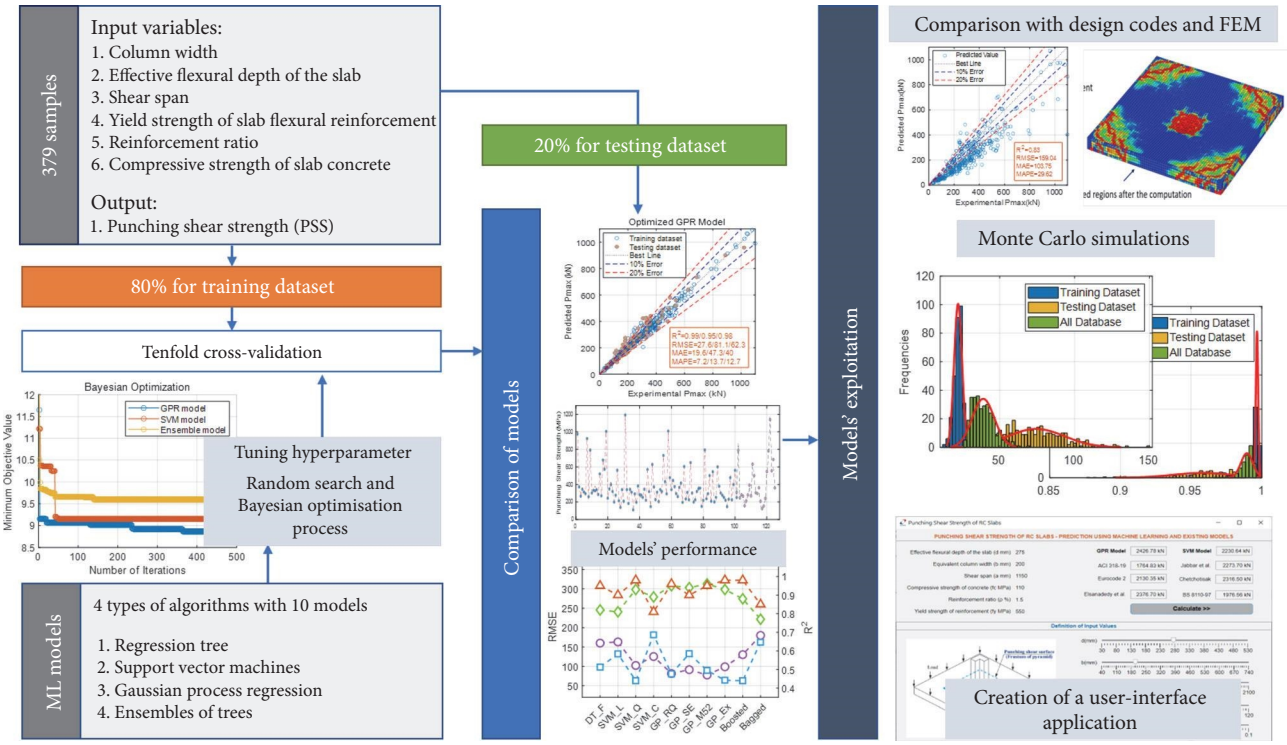

Figure 1: Outline of the research work.

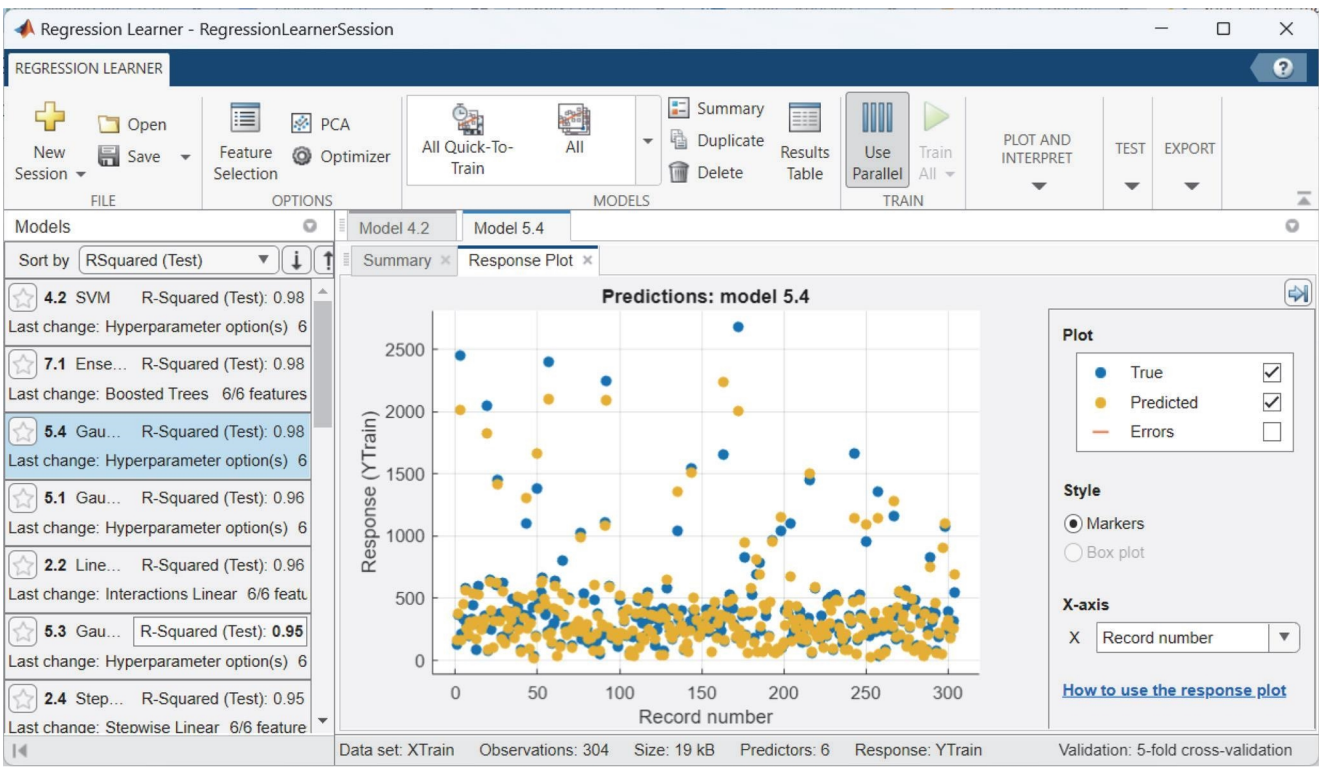

Figure 2: Performance evaluation and results from our study using machine learning models developed with the MATLAB's Regression Learner app.

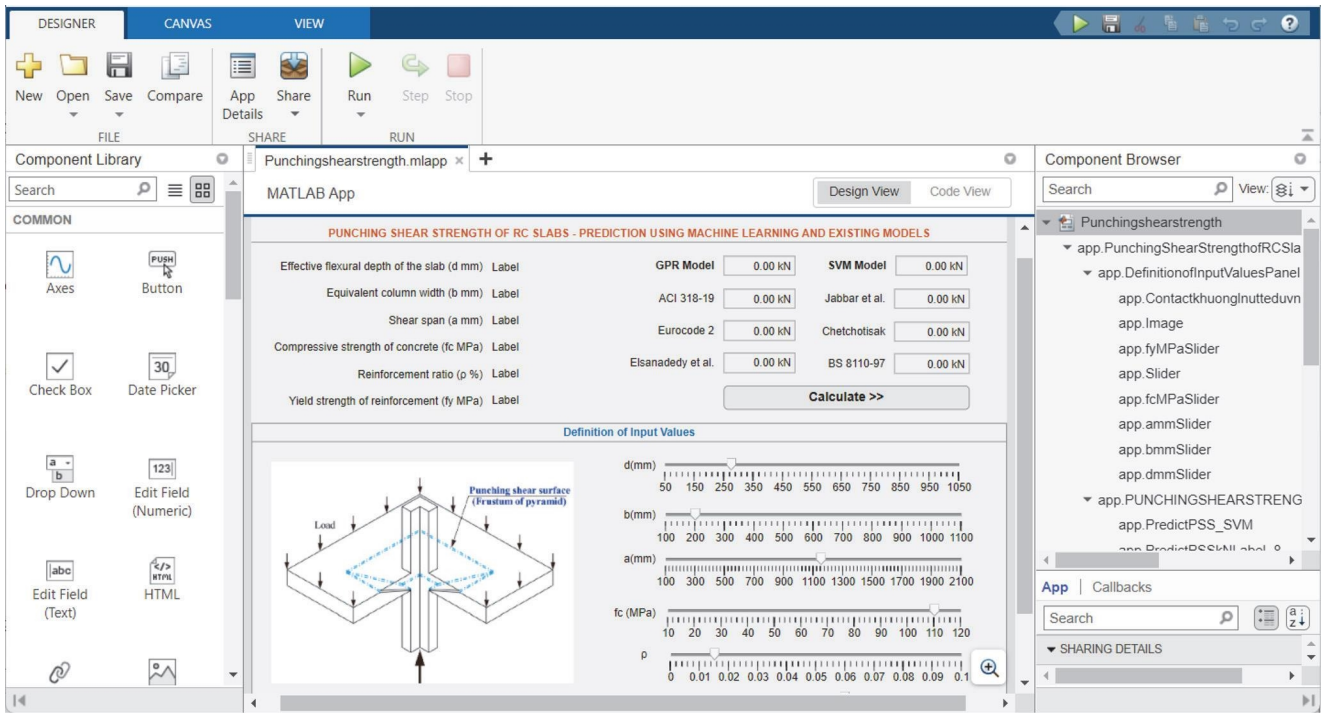

Figure 3: The integrated user interface of the MATLAB's App Designer application used in this study.

various components of this app, as they pertain to this research, are depicted in Figure 3.

2.2. ML Models Description. This study utilised four ML models integrated within MATLAB's Regression Learner app: decision tree, SVMs, GPR, and ensemble of trees. Decision tree is a tree-based model that can handle nonlinear relationships between the input variables and target outputs [20]. SVMs can transform the target variable into a continuous one and identify the hyperplane maximising the margin between distinct data classes [21]. Ensemble of trees, also known as tree ensembles or tree-based methods, is a powerful ML technique that involves constructing multiple decision trees and combining their outputs to achieve improved performance. By aggregating the predictions of multiple trees, the ensemble model can overcome the limitations of individual trees, such as overfitting and instability, and achieve higher accuracy and robustness [22]. GPR [11] is a Bayesian model using Gaussian distributions to represent relationships between the input variables and target outputs, modelling complex, nonlinear relationships and providing uncertainty estimates for its predictions.

The Regression Learner app in MATLAB offers a rich selection of model options across four ML algorithms, expanding the possibilities for users to tailor the models to their specific needs. Depending on the nature of the data and the type of problem to be solved, users can adjust the complexity and functionality of their models to optimise performance.

In the realm of SVM models, users can select from linear, quadratic, or cubic options, each representing a different level of complexity in the input–output relationship. For problems with linear correlations, the linear SVM might be an ideal choice, while quadratic or cubic SVMs could be more suitable for nonlinear, complex patterns.

The decision tree algorithm also presents diverse options, allowing users to choose between trees of varying complexity levels. For instance, binary trees might be suitable for simpler, binary classification problems, while regression trees can handle more nuanced, continuous data.

In the GPR model, users have the flexibility to choose from different kernels, each representing a distinct way of capturing the input–output relationship. Varieties include the rational quadratic, squared exponential, matern 5–2, and exponential kernels, each with their unique characteristics and ideal use cases.

Ensemble of trees models, on the other hand, provide an opportunity to leverage the power of multiple learners. Users can opt for ensemble methods such as bagging or boosting, which can enhance model accuracy by aggregating predictions from multiple decision trees.

The flexibility and diversity of these models help users navigate the complex landscape of ML, enabling them to identify and implement the most suitable model for their specific needs. Table 1 encapsulates these considerations, summarising the key features of each model type, the specific models, the acronyms used in this research, and the notable hyperparameters. It provides a comprehensive view of the range of models employed in this research, showcasing the versatility and utility of the Regression Learner app in MATLAB for tackling complex engineering problems.

2.3. Evaluating Model Performance Metrics. This study employed four statistical parameters to evaluate the accuracy of the proposed model, namely correlation coefficient (R),

Table 1: Integrating the detailed information about the specific models used in the study.

	Model type	Model	Acronym used for this research	Hyperparameters
1	Decision tree	Fine tree regression	DT_F	Minimum leaf size Surrogate decision splits
2	Support vector machines	Linear SVM	SVM_L	Kernel function
3		Quadratic SVM	SVM_Q	Kernel scale
4		Cubic SVM	SVM_C	Box constraint Epsilon
5	Gaussian process expression	Rational quadratic	GP_RQ	Basic function
6		Squared exponential	GP_SE	Kernel function
7		Matern 5–2	GP_M52	Isotropic kernel
8		Exponential	GP_Ex	Kernel scale Signal standard deviation Sigma
9	Ensembles of trees	Boosted trees	Boosted	Minimum leaf size
10		Bagged trees	Bagged	Number of learners Learning rate

root-mean-square error (RMSE), mean absolute error (MAE), and mean absolute percentage error (MAPE). The forecasting model's quality improves as the MAPE, RMSE, and MAE values decrease. On the other hand, R indicates the degree of correlation between the actual and predicted values, ranging from 0 to 1, where higher values of R indicate better-performing models. The mathematical formulations for the three statistical indexes are as follows:

MAE

$$\mathrm{MAE} = \frac{1}{N}\sum_{j=1}^{N}\left|p_j - p_{t,j}\right|, \tag{1}$$

RMSE

$$\mathrm{RMSE} = \sqrt{\frac{1}{N}\sum_{1}^{N}\left(p_j - p_{t,j}\right)^2}, \tag{2}$$

Correlation coefficient

$$R^2 = \left[\frac{\sum_1^N\left(p_j - \overline{p}\right)\left(p_{t,j} - \overline{p_t}\right)}{\sqrt{\sum_1^N\left(p_j - \overline{p}\right)^2\sum_1^N\left(p_{t,j} - \overline{p_t}\right)^2}}\right]^{1/2}, \tag{3}$$

MAPE

$$\mathrm{MAPE} = \frac{100\%}{N}\sum_{j=1}^{N}\left|\frac{p_j - \mathrm{p}_{t,j}}{p_j}\right|, \tag{4}$$

where p_j is the PPS of jth actual value in the dataset; $p_{t,j}$ is the PPS of jth predicted value obtained from ML model; $\overline{p}$ is the mean actual value of the PPS compliance; $\overline{p}_t$ is the mean predicted value of the PPS; and N is the total number of samples in the dataset.

2.4. FEM- for RC Slab Simulation. In this investigation, a nonlinear 3D finite-element analysis (FEA) approach was employed to determine the punching shear of slabs. The modelling technique was implemented using the open-source programme Cast3M [23], and a detailed discussion of the methodology can be found in a previous research publication [16]. The key components of the process can be summarised as follows:

Meshing and elements: the RC slabs were represented using 3D isoparametric elements. These elements, each having eight nodal points, were configured with dimensions of 25 mm × 25 mm × 20 mm (length × width × thickness). This choice ensured a detailed representation of the slab geometry while optimising computational efficiency.

Boundary conditions: to simulate the realistic constraints of the slabs in their operational environment, displacements were restricted to the vertical direction. This boundary condition mimicked real-world scenarios where primary displacements under loading occur vertically.

Material properties: the nonlinear behaviour of concrete was captured using the Mazars [24] 3D damage concrete model. This model, rooted in damage theory, characterises material degradation via a damage parameter which signifies microcracking states. For enhanced accuracy, an improved version of this model [25] was incorporated, introducing different internal variables in representing shear behaviour of concrete.

Analysis procedure: the PASAPAS process integrated within Cast3M was utilised for a static pushover analysis. By superimposing a displacement atop the slab's column area, a pushover curve was generated, representing the relationship between load and displacement. The peak value on this curve provided the slab's PSS.

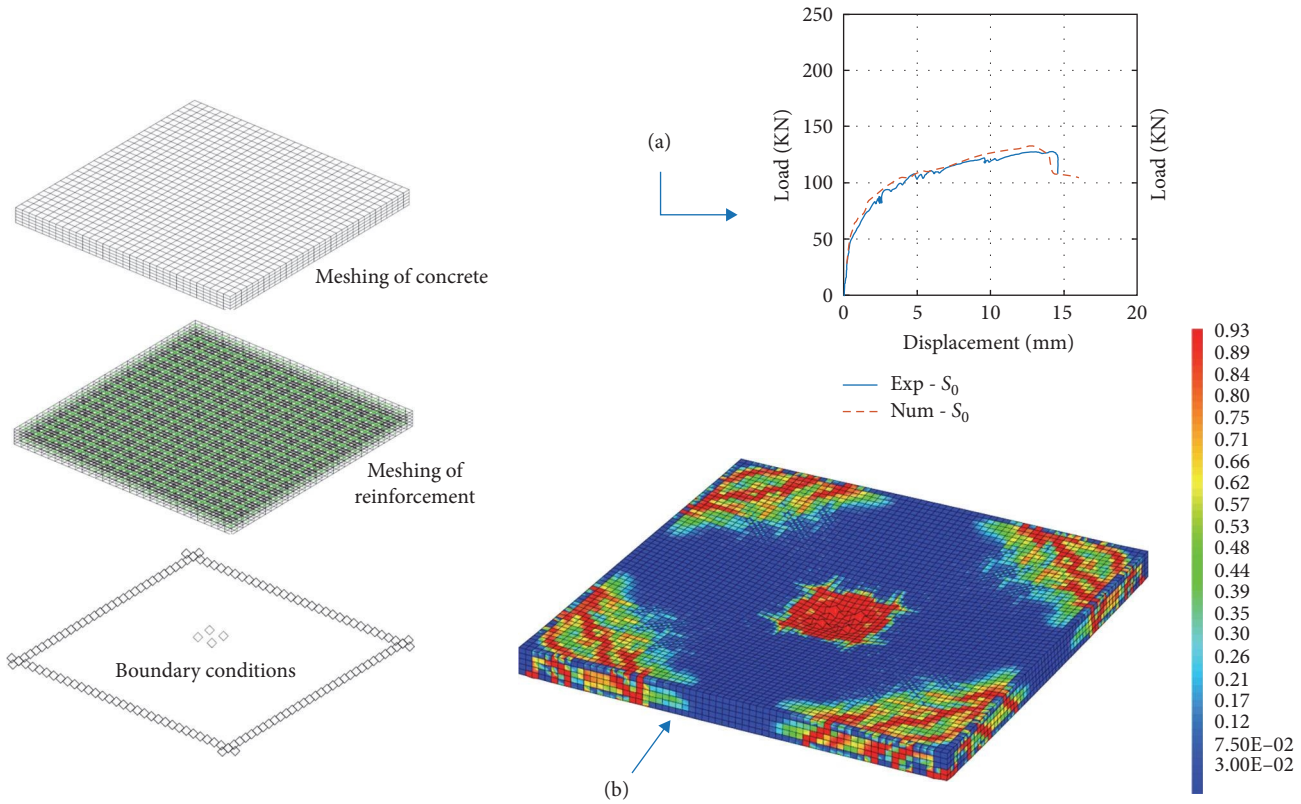

Figure 4: A nonlinear pushover analysis example for calculating the punching shear of RC slabs. (a) Pushover analysis comparison between experimental and numerical; and (b) damaged regions after the computation.

Figure 4 provides a detailed illustration of the computational process employed in this study. To achieve accurate results, the concrete Mazars model's input parameters were scrupulously calibrated to align the pushover curve with data obtained from numerical simulations and experimental measurements, as outlined in the research conducted by Le-Nguyen et al. [16]. In order to facilitate the analysis, boundary conditions were established to restrict displacement solely in the vertical direction. A comprehensive comparison of the pushover analysis between experimental and numerical outcomes is presented in Figure 4(a). Furthermore, Figure 4(b) displays the damaged regions at the failure strength of the specimen, providing valuable insights into the structural behaviour under the applied loading conditions.

3. Data Description

All algorithms were implemented in open-source frameworks, utilising 379 experimental data points gathered from 53 experimental works [26–78] and are summarised in Table 2. The data used in this research were meticulously selected to eliminate the influence of variable diversity effects, such as the presence of fibre-reinforced plastic reinforcement, bond failure, or specimens lacking shear spans. Consequently, only specimens exhibiting brittle punching shear failure were considered for inclusion in the dataset. The input variables consist of the compressive strength of the slab concrete (f_c), yield strength of the slab flexural reinforcement (f_y), equivalent column width (b), effective flexural depth of the slab (d), shear span (a), and slab reinforcement ratio (ρ). The target output variable is the PSS. Within the current database, there are 222 square slabs, 108 round slabs, 35 rectangular slabs, and five octagonal slabs; slab profiles for the remaining nine specimens are not available. Moreover, the columns used in the models have three cross-sectional shapes: 207 square columns, 144 round columns, and 28 rectangular columns.

Table 2: Properties of input parameters.

Parameter	Mean	Min.	Median	Max.	Std.
b (mm)	181.42	40.06	173.57	707.64	92.39
d (mm)	112.91	30.00	107.00	500.00	58.30
a (mm)	648.16	38.00	675.00	2320.00	318.60
ρ (%)	1.26	0.33	1.11	3.73	0.66
f_y (MPa)	469.79	250.00	471.00	749.00	118.28
f_c (MPa)	32.87	8.66	28.00	118.70	18.51
P_{max} (MPa)	379.02	24.00	282.50	2681.00	387.18

Table 2 and Figure 5 provide important information about the range and distribution of the variables used in the study. The study encompasses a diverse range of RC slab configurations and material properties. The equivalent column width (b) has a mean value of 181.42 mm and a standard deviation of 92.39 mm, indicating a wide variety of column widths. The effective flexural depth (d) displays

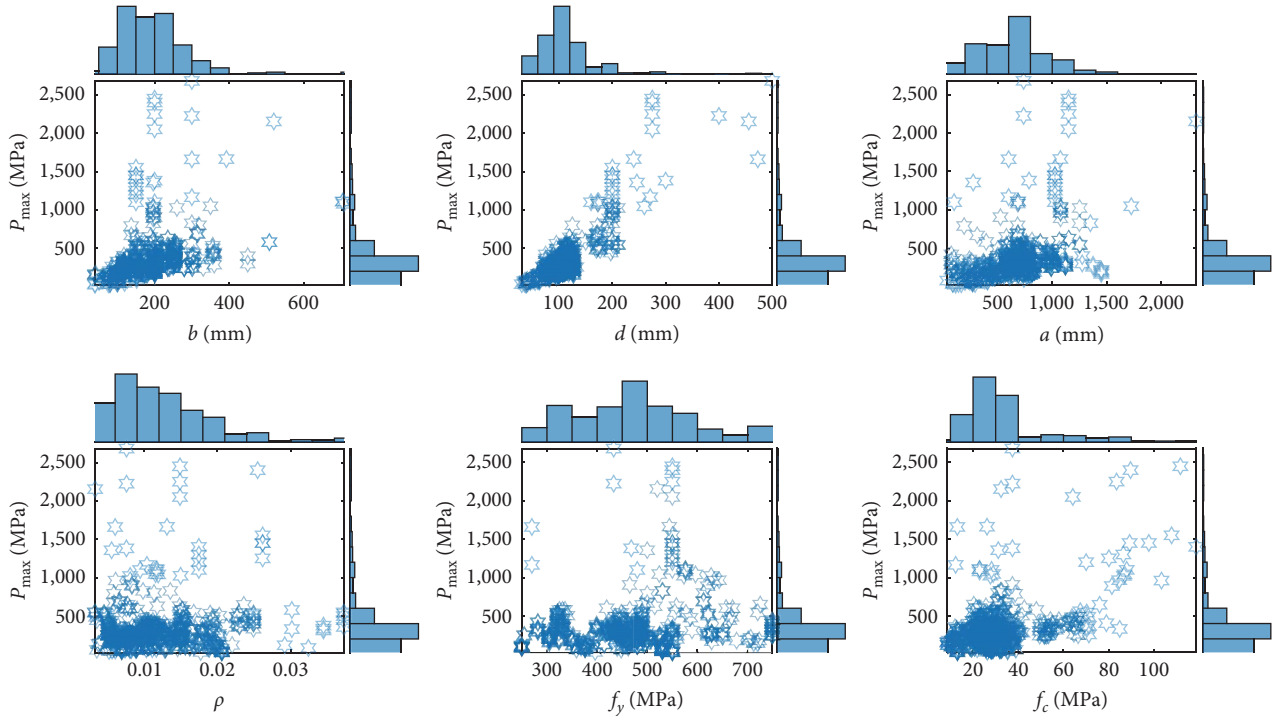

Figure 5: Distribution of the parameters.

a mean value of 112.91 mm and a standard deviation of 58.30 mm, showcasing the diversity in slab depths. The shear span (a) has a mean value of 648.16 mm and a standard deviation of 318.60 mm, reflecting the various shear spans included in the dataset. The slab reinforcement ratio (ρ) has a mean value of 1.26% and a standard deviation of 0.66%, indicating the range of reinforcement ratios considered. The yield strength of the slab flexural reinforcement (f_y) demonstrates a mean value of 469.79 MPa and a standard deviation of 118.28 MPa, highlighting the variety of reinforcement strengths in the dataset. The compressive strength of the slab concrete (f_c) has a mean value of 32.87 MPa and a standard deviation of 18.51 MPa, suggesting a broad range of concrete strengths used in the study. Finally, the maximum load applied to the slab (P_{max}) features a mean value of 379.02 MPa and a standard deviation of 387.18 MPa, emphasising the diverse loading conditions considered in the research.

4. Machine Learning Implementation and Results

4.1. Evaluating ML Models with Default Hyperparameters. The performance of the models was evaluated using the ten-fold cross-validation approach. The validation dataset that was produced by this method was utilised for both hyperparameter tuning and model assessment. Figure 6 comprehensively evaluates the performance of various ML models across three datasets: training set, validation, and testing set. These models include decision tree (DT_F), SVMs with linear kernel (SVM_L), quadratic kernel (SVM_Q), cubic kernel (SVM_C), Gaussian process with rational quadratic kernel (GP_RQ), squared exponential kernel (GP_SE), matern 5/2 kernel (GP_M52), exponential kernel (GP_EX), Boosted, and Bagged. The performance metrics assessed for each model are AE, mean squared error (MSE), RMSE, and R-squared (R^2).

Upon analysing the results, it is evident that the models display varying performance levels across the three datasets. The Gaussian process with exponential kernel (GP_EX) demonstrates exceptional performance on the training set, with the lowest MAE (4.5), MSE (67.8), and RMSE (8.2) values, as well as the highest R^2 (1.00) value. This result suggests that the GP_EX model is highly accurate and possesses strong predictive capabilities when applied to the training set.

In contrast, the SVM with a linear kernel (SVM_L) exhibits relatively weaker performance, particularly in the validation and testing sets. The model records high values for MAE, MSE, and RMSE, while its R^2 values remain consistently lower than those of other models. Notably, the Bagged model demonstrates consistently moderate performance across all datasets. While it does not outperform the other models in any specific category, it maintains relatively stable results, indicating that it may be reliable when applied to a diverse range of data.

Identifying a suitable model is vital as it guarantees improved predictive accuracy and enables efficient generalisation to previously unseen data. Ultimately, this meticulous selection process produces dependable insights, fostering informed decision-making within the context of the given problem. As the research advances, subsequent efforts will be devoted to refining the existing models to bolster their

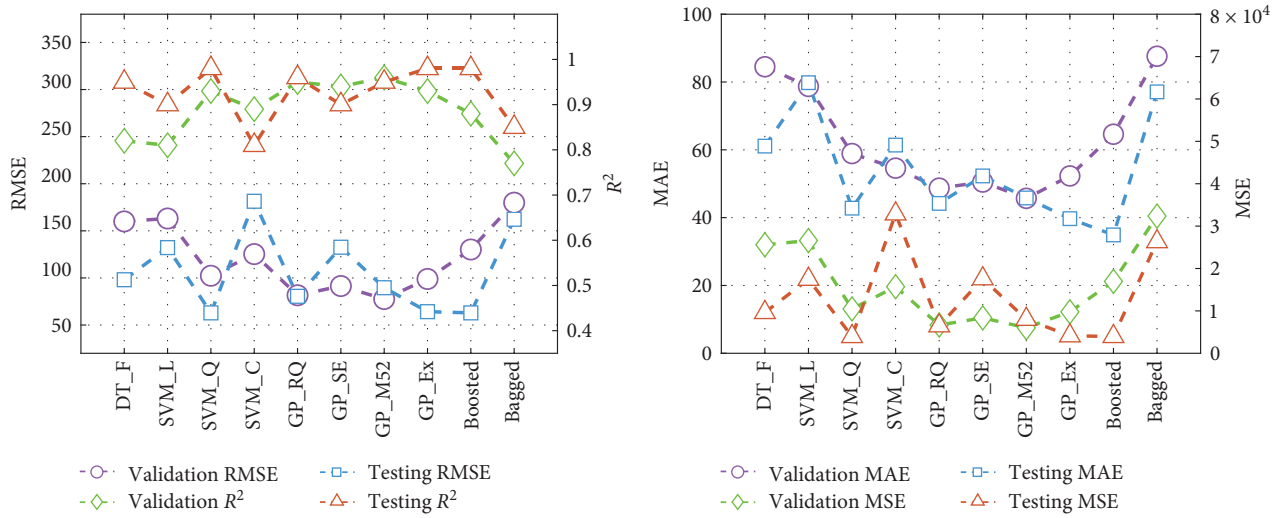

Figure 6: Comparison of R^2 values between models for validation and test sets.

performance. This optimisation process, which involves fine-tuning the hyperparameters, has been carried out accordingly.

4.2. Assessing Model Performance with Optimised Hyperparameters. Hyperparameter tuning is a crucial step in the ML model training process as it helps in finding the optimal combination of hyperparameters that results in the best performance of the model. In this research, two methods were used for hyperparameter tuning, namely random search and the Bayesian optimisation process. The Bayesian optimisation method intelligently explores the hyperparameter space, using a Gaussian process surrogate model to predict the performance of different parameter combinations, while the random search method samples the hyperparameter space randomly to find the best combination. These two complementary methods, embedded within the Regression Learner app, enable users to enhance model performance with minimal effort, thus showcasing the effectiveness of low-code tools for practical machine-learning applications.

Table 3 displays the range of values and the optimised values chosen from the hyperparameter tuning process. These optimised values will be utilised to make predictions in the final models. By utilising both Bayesian optimisation and random search, it is anticipated that the models will achieve improved accuracy in predicting PSS compared with models with default hyperparameters.

A total of 500 iterations were applied for the hyperparameter tuning process for each method to ensure the robustness of the results. Figure 7 illustrates the minimum mean squared error (MSE) convergence curve for three models obtained through Bayesian optimisation and random search processes, with MSE values computed using a tenfold cross-validation technique. The GPR model with optimised hyperparameters performs better than the other models. Although the MSE values after 500 optimal iterations for all models are approximately equal using both tuning methods, the convergence rate differs, with Bayesian optimisation converging after roughly 150 iterations and the random search process converging faster at around 100 iterations. This observation suggests that the random search process achieves convergence more rapidly than Bayesian optimisation, offering an advantage in terms of computational efficiency and resource usage. The differing performance may be attributed to factors such as data nature, model complexity, or the optimiser used. While Bayesian optimisation may be too conservative, leading to suboptimal results, random search can explore diverse hyperparameters but risks overfitting or poor generalisation.

Figure 8 presents the best R^2 and RMSE scores of GPR, SVM, and ensemble models with varying hyperparameters across the training, validation, and testing datasets. The results show that the performance improvement in models with optimised hyperparameters is not substantially greater than those with default hyperparameters. In other words, the models with default hyperparameters, such as the GPR model with rational quadratic, squared exponential, matern 5–2, or exponential kernel, suggested by the Regression Learner app, can already yield satisfactory results without the need for any hyperparameter tuning process.

This observation underscores the advantages of utilising low-code tools, such as MATLAB's Regression Learner app, in practical applications. These tools enable users to quickly develop and deploy ML models with minimal effort, as they can provide satisfactory results even without extensive hyperparameter optimisation. This is particularly beneficial when computational resources are limited or rapid prototyping is required.

However, it should be noted that the performance of default hyperparameters may not always be optimal, and further optimisation could still lead to improved results in specific cases. Moreover, different models may be more sensitive to hyperparameter tuning, and the degree of improvement may vary accordingly. Therefore, while low-code tools like the Regression Learner app offer valuable convenience and a practical starting point, it remains crucial to consider

Table 3: Hyperparameters with tuning range and optimal values.

Model	Hyperparameter name	Range	Optimal value using Bayesian process	Optimal value using random search
GPR	"Sigma"	[1.00e−04,3.78e + 03]	41.401	38.7
	"BasisFunction"	"constant" "none" "linear" "pureQuadratic"	"linear"	"none"
	"KernelFunction"	"ardmatern32" "ardmatern52" "exponential" "matern32" "matern52" "squaredexponential"	"matern32"	"matern32"
	"KernelScale"	(1.6870, 1,687)	7.329	18.3
	"Standardise"	"true" "false"	"true"	"true"
SVM	"BoxConstraint"	(1.00e−03, 1,000)	83.518	68.53
	"Epsilon"	(0.165, 1.65e + 04)	0.293	0.282
	"KernelFunction"	"gaussian" "linear" "polynomial"	"polynomial"	"polynomial"
	"PolynomialOrder"	[2, 4]	2	2
	"Standardise"	"true" "false"	"true"	"true"
Ensemble	"Method"	"Bag "LSBoost"	"LSBoost"	"LSBoost"
	"NumLearningCycles"	(10,500)	487	497
	"LearnRate"	(1.00e−03,1)	0.049	0.035
	"MinLeafSize"	(1,152)	2	4
	"MaxNumSplits"	(1,303)	5	103
	"NumVariablesToSample"	[1, 6]	5	4

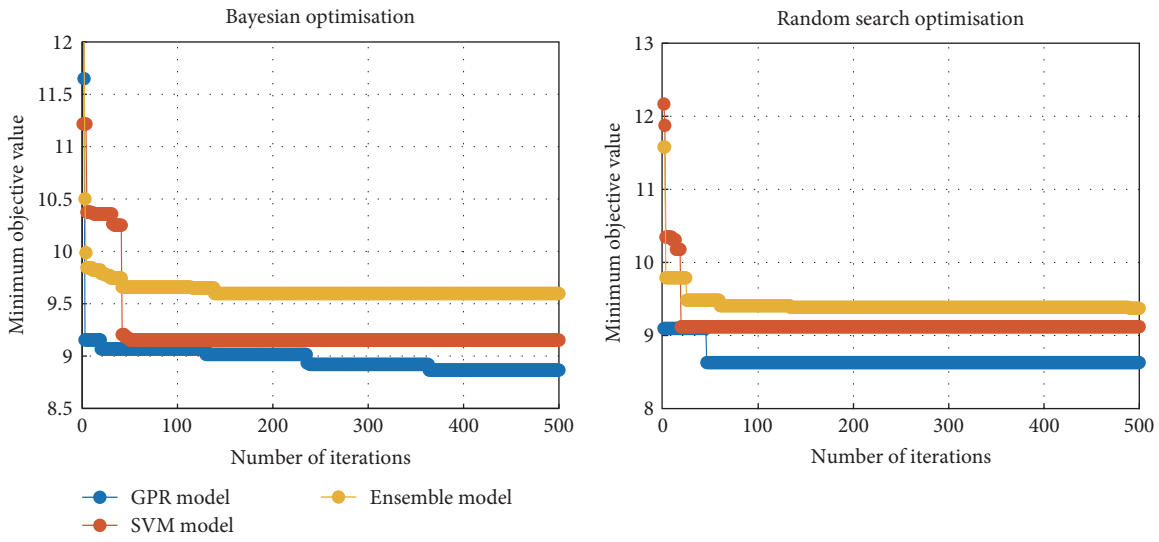

Figure 7: Minimum MSE converged curve using Bayesian optimisation and random search process.

the potential benefits of hyperparameter optimisation for enhancing model performance and robustness in various applications.

4.3. Examining Representative Prediction Results. Table 4 presents a performance metrics comparison of ML models with different tuning methods. Among the models with tuned hyperparameters, the GPR model consistently performed well across all sets and optimisation methods, exhibiting R^2 values of 0.995, 0.954, and 0.978 on the training, validation, and testing sets, respectively. The SVM model also demonstrated strong performance, with R^2 values of 0.955, 0.933, and 0.973 using Bayesian optimisation and 0.955, 0.926, and 0.974 using random search.

Conversely, the ensemble model excelled on the training set, with R^2 values of 0.997 and 0.999 using Bayesian

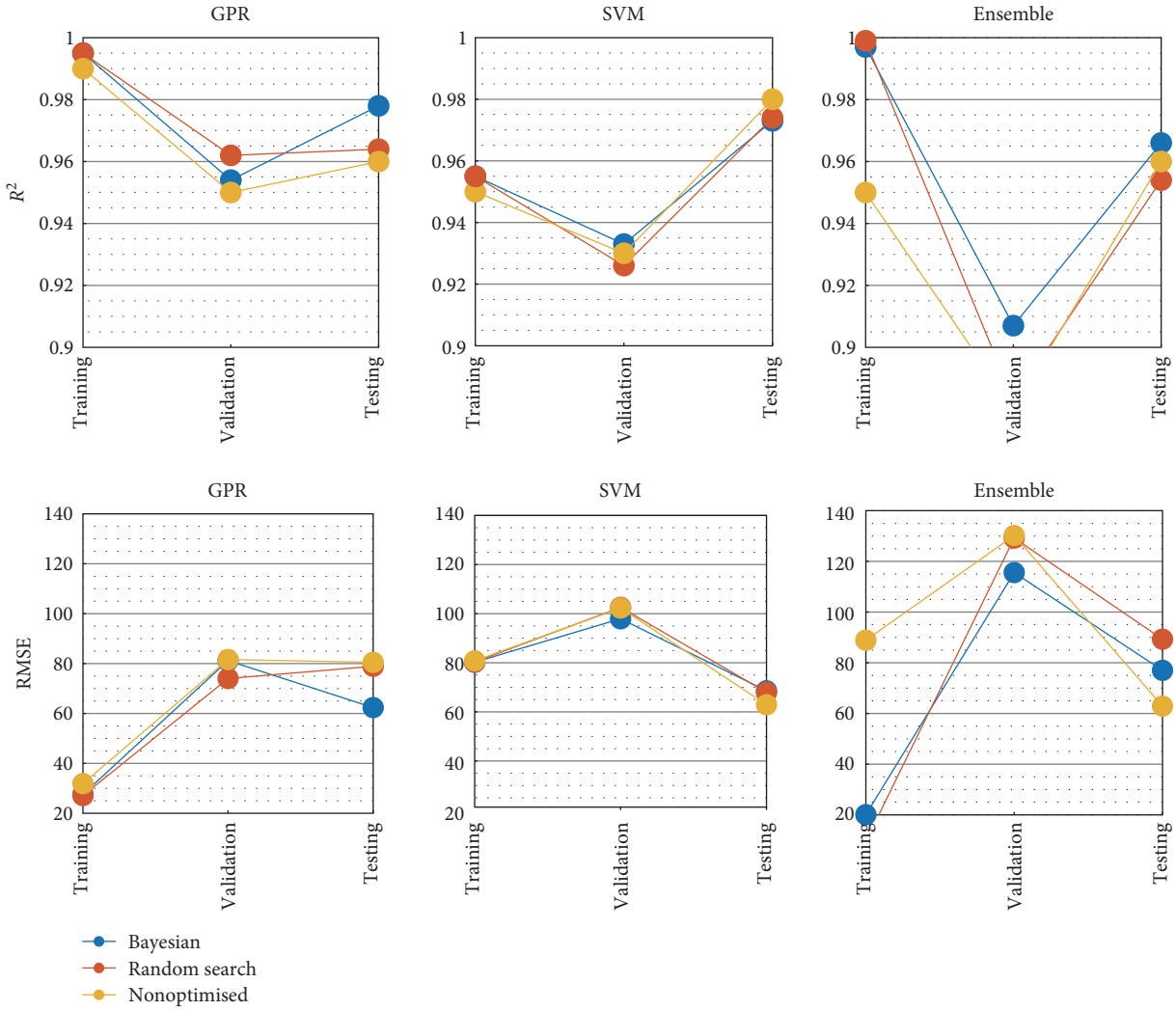

Figure 8: Best R^2 and RMSE scores of GPR, SVM, and ensemble models with different hyperparameters on training, validation, and testing.

optimisation and random search, respectively. However, it exhibited relatively lower performance on the validation and testing sets, with R^2 values of 0.907, 0.883, and 0.966.

Overall, models with optimised hyperparameters display a better balance between training and testing performance, suggesting a reduced risk of overfitting or underfitting. In comparison, models with default hyperparameters, such as the ensemble model with default settings, show higher error metrics and lower R^2 values on validation and testing sets, indicating potential overfitting issues.

Figure 9 presented a comparison of experimental values and predicted PSS for flat slabs without transverse reinforcement using GPR and SVM models with optimised hyperparameters. In this figure, the dashed lines represent experimental values, while dots depict the predicted values by the models. To enhance the presentation, each data point displayed is calculated as the average of the PSS for four consecutive data samples.

The results showcased in the figure indicate that the punching resistance of experimental samples in the training dataset closely aligns with the model's predictions. Similarly, using the testing database, experimental results are also predicted with minimal error. The accuracy of the models is further assessed through the evaluation of error values and the regression charts comparing experimental data and predicted results for both GPR and SVM models. This thorough analysis emphasises the high performance and precision of the developed models when applied to flat slabs without transverse reinforcement.

4.4. Analysing the Influence of Data Randomness through Monte Carlo Simulation. Integrating Monte Carlo simulations with the hold-out method for generating distinct training and testing datasets is a crucial step in evaluating the generalizability of the ML models. Several earlier investigations have emphasised the influence of the random sampling process on a model's predictive performance [79]. Therefore, to ensure the model's reliability, a significant number of simulations must be executed before employing it to validate the findings' generalizability.

In this study, a total of 600 Monte Carlo simulations are performed across four different models. The results, in terms

Table 4: Performance metrics comparison of machine learning models with different tuning methods.

Model	Set	MAE	RMSE	R^2
GPR model with Bayesian optimisation	Training set	19.61	27.59	0.995
	Validation	47.34	81.19	0.954
	Testing set	40.04	62.36	0.978
SVM model with Bayesian optimisation	Training set	46.46	80.24	0.955
	Validation	58.7	97.91	0.933
	Testing set	44.74	68.57	0.973
Ensemble with Bayesian optimisation	Training set	15.04	20.09	0.997
	Validation	54.94	115.57	0.907
	Testing set	43.87	77.01	0.966
GPR model with random search tuning	Training set	19.05	27.09	0.995
	Validation	43.58	74.01	0.962
	Testing set	42.47	78.908	0.964
SVM model with random search tuning	Training set	46.47	80.3	0.955
	Validation	58.92	102.57	0.926
	Testing set	44.58	67.97	0.974
Ensemble model with random search tuning	Training set	3.29	9.58	0.999
	Validation	56.78	129.19	0.883
	Testing set	47.98	89.29	0.954
SVM model with quadratic kernel	Training set	47.8	80.8	0.95
	Validation	58.9	102.3	0.93
	Testing set	42.8	62.9	0.98
GPR with rational quadratic kernel	Training set	22.8	31.9	0.99
	Validation	48.7	81.6	0.95
	Testing set	44.2	80.5	0.96
Ensemble model with default hyperparameters	Training set	44.6	88.9	0.95
	Validation	64.6	130.2	0.88
	Testing set	34.9	62.9	0.96

of R^2 and RMSE values for each model, are obtained from 300 separate simulations and are presented in histogram plots in Figure 10(a) for the GPR model and Figure 10(b) for the SVM model. These plots provide a visual representation of the distribution of R^2 and RMSE values, offering insights into the models' performance and their robustness against variations in the data.

The training dataset, testing dataset, and the entire database are all utilised for evaluation purposes, which enables a comprehensive assessment of the accuracy of the algorithms' predictions. Among the four optimised models, all exhibit an R^2 value for the testing dataset of ∼0.98, indicating a high level of accuracy in predicting the target variable. However, the GPR model stands out with the most favourable results, achieving an R^2 value of around 0.99 for all databases. This highlights the superior predictive capability of the GPR model compared to the other models.

Furthermore, the consistency of the R^2 values across various datasets suggests that the developed models are not sensitive to the data hold-out method, which is a critical aspect of their generalizability. In particular, the GPR model demonstrates stability and robustness against changes in the data, ensuring reliable performance in various scenarios. This finding underscores the potential of the GPR model as a valuable tool for predicting the target variable, even when faced with variations in the data or potential uncertainties in real-world applications.

5. Practical Implications

5.1. Comparing ML Model Performance with Practical Codes and FEM Simulations. In this study, the accuracy and reliability of the GPR model developed were validated by comparing its performance against multiple benchmarks. The performance of the GPR model was compared with three commonly used current design codes, three empirical equations proposed by other researchers, and FEM simulations.

Three design codes were studied, including ACI 318-19 [80], EC2 [81], BS 8110-97 [82], and three empirical equations by Jabbar et al. [83], Chetchotisak et al. [7], and Elsanadedy et al. [84]. The equations for the design codes and the empirical equations utilised for the comparative study may be found in Table 5.

As discussed in the Section 2.4, the FEM simulations in this study were performed using the nonlinear pushover technique and were automated using MATLAB-Cast3M. However, if a nonconverged problem occurred during the simulation, the outcome was deemed "not successful". For

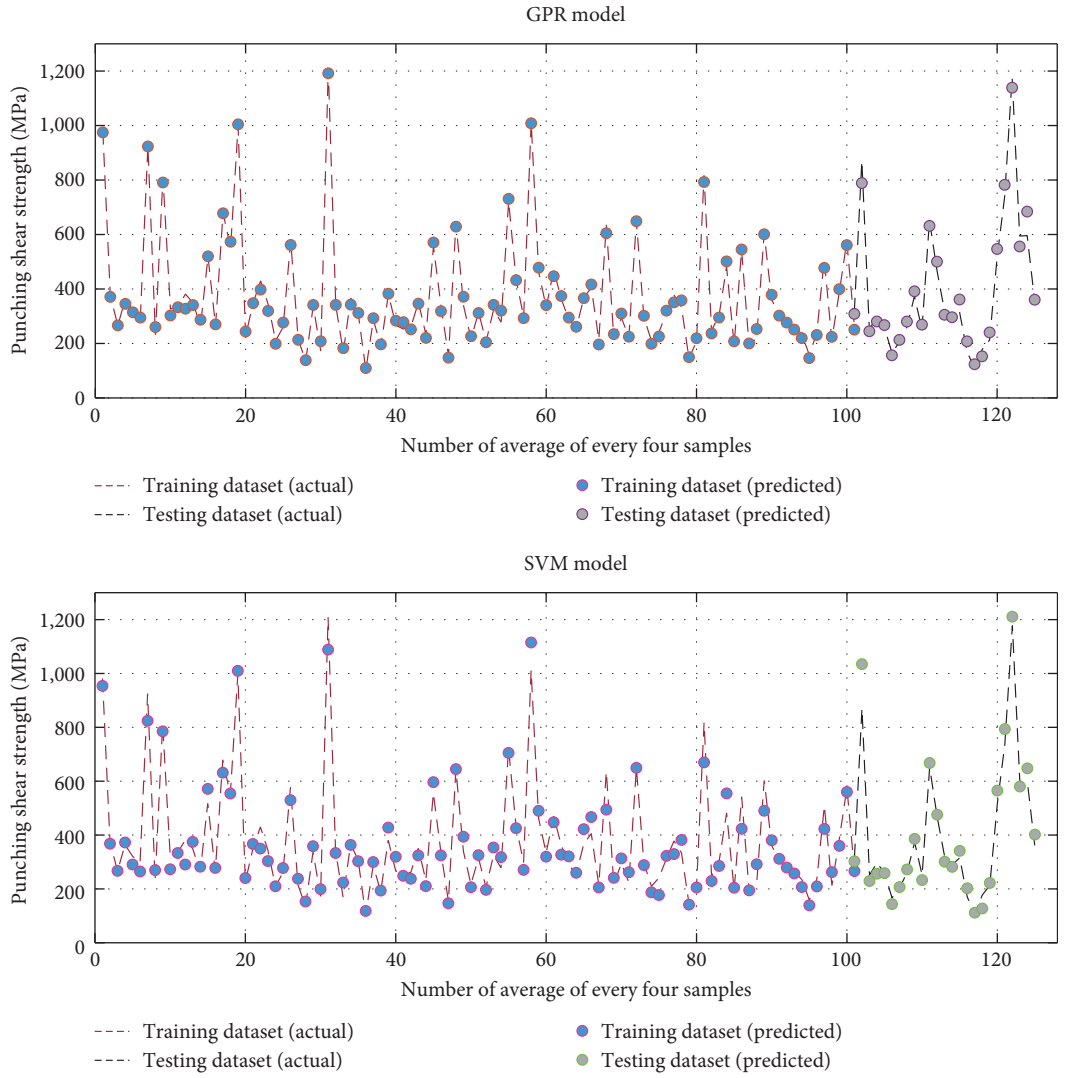

FIGURE 9: Predicted and experimental of punching shear strength values for the training database and testing database.

the "successful" simulations, the maximum reaction value obtained during the Pushover process was considered the PSS of the slab. Out of the 379 simulations performed, only 227 were able to calculate the PSS without experiencing a nonconverged problem.

The regression model depicts the relationship between the actual experimental values and the predicted values from ACI 319-19 (Figure 11(a)), EC2 (Figure 11(b)), BS 8110-97 (Figure 11(c)), Jabbar's model (Figure 11(d)), Chetchotisak's model (Figure 11(e)), Elsanadedy's model (Figure 11(f)), FEM (Figure 11(g)), and GPR model with optimised hyperparameters (Figure 11(h)) for both training and testing datasets. The horizontal axis represents the measured PSS of the specimens, while the vertical axis indicates the predicted PSS.

The best-fit line signifies the ideal condition where the predicted values are equal to the tested values. The blue and red dashed lines represent the 10% and 20% error contours, respectively, providing a clear indication of the deviation from the ideal prediction. The proposed model exhibits near-perfect performance with the training dataset, as the majority of data points closely align with the $y = x$ line, indicating a high degree of accuracy in the predictions.

In addition, Table 6 summarises the statistical criteria values of design codes and empirical formulas in predicting the PSS of flat slabs without transverse reinforcement. ACI 319-19, EC2, and BS 8110-97 are well-established design standards that provide reasonably accurate predictions, with R^2 values of 0.831, 0.934, and 0.937, respectively. However, their error metrics, particularly MAE and MAPE, are relatively high compared to the other methods. Jabbar et al. [83], Chetchotisak et al. [7], and Elsanadedy et al. [84] are alternative models that show improved performance with R^2 values around 0.93 and lower error metrics compared to the design standards. FEM simulations (227/379 predictions) exhibit exceptional performance, with an R^2 value of 0.999 and significantly lower error metrics compared to all other methods. However, as previously discussed, FEM simulations can be computationally demanding and time-consuming, which may limit their practical applications. The GPR model shows impressive performance with an R^2

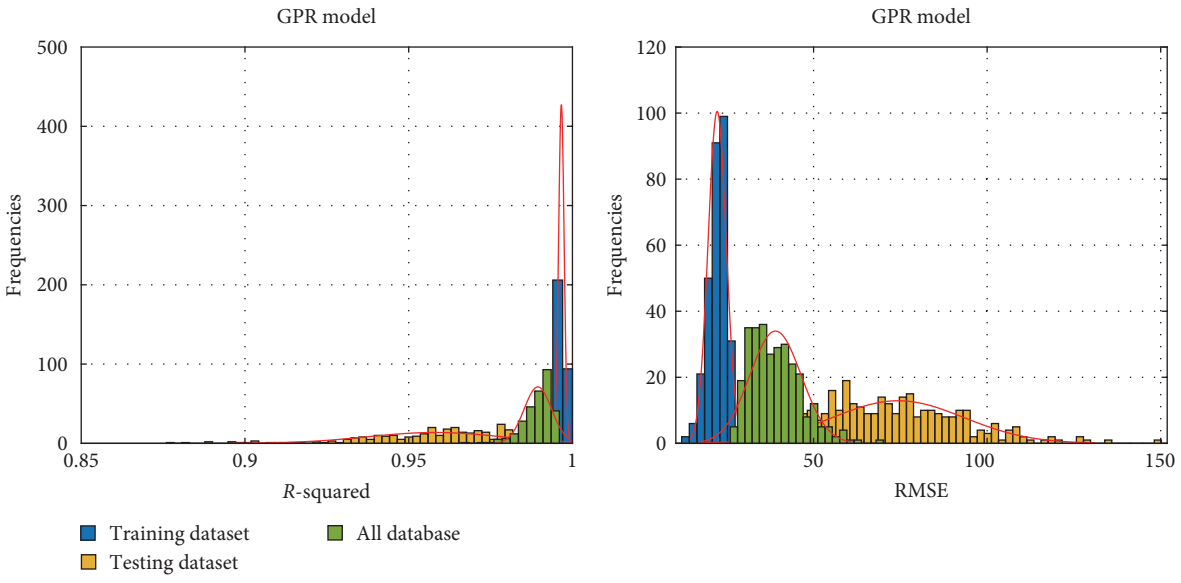

Figure 10: Histogram of performances of 300 Monte Carlo simulation of (a) GPR and (b) SVM model.

value of 0.996 and lower error metrics compared to the design standards and alternative models. It demonstrates a good balance between accuracy and computational efficiency, making it an attractive choice for practical applications.

Upon analysing the results, it becomes evident that the FEM simulation and GPR models demonstrate the best performance on the testing dataset, confirming their outstanding predictive capabilities when compared to the other methods. This superior performance can be attributed to the optimised hyperparameters of the GPR model and the advanced computational abilities of the FEM simulation, which enable them to accurately capture the complex relationships within the data. Consequently, the optimised FEM simulation and GPR models emerge as reliable and effective tools for predicting the PSS of flat slabs without transverse reinforcement, outperforming other established models and design codes in this regard.

While both the FEMFEM simulation and the GPR model with optimised hyperparameters exhibit exceptional performance in predicting the PSS of flat slabs without transverse reinforcement, it is important to consider the time consumption and practicality of each method for real-world applications.

FEM simulations are known to be computationally demanding and time-consuming due to the high level of detail and complexity involved in the process. This can be a significant drawback in practical applications, particularly

Table 5: Empirical models in the literature.

Reference	Equation
ACI 318-19 [80]	$V_n = \min\left[\left(0.17\left(1+\frac{2}{\beta}\right)\lambda_s,\ 0.083\left(\frac{\alpha_s d}{B_0}+2\lambda_s\right),\ 0.33\lambda_s\right)\sqrt{f_c}B_0 d\right]$ $B_0 = 4(b+d)$ $\lambda_s = \sqrt{\frac{2}{1+0.004d}} \le 1$ $\alpha_s = 40$ for interior columns; $\alpha_s = 30$ for edge columns; and $\alpha_s = 20$ for corner columns
EC2 [81]	$V_n = 0.18\zeta(100\rho f_{ck})^{\frac{1}{3}}B_0 d$ $\zeta = \left(1+\frac{200}{d}\right) \le 2$ $f_{ck} = f_c - 1.6$ $B_0 = 4(b+\pi d)$
BS 8110-97 [82]	$V_n = 0.79\zeta\left(100\rho\frac{f_{cu}}{25}\right)^{\frac{1}{3}}B_0 d$ $\zeta = \left(\frac{400}{d}\right)^{\frac{1}{4}}$ $B_0 = 4b + 12d$
Jabbar et al. [83]	$V_n = 0.9\sqrt[3]{f_c}\sqrt[4]{\frac{200}{d}}\sqrt{f_y\rho}B_0 d\sqrt{\frac{d}{B_0}}$ $B_0 = 4(b+d)$
Chetchotisak et al. [7]	$V_n = 92.43(f_c)^{1.21}\left(\frac{1}{100\rho}\right)^{1.47}(B_0)^{0.42}d^{1.35}\zeta^{4.66}$ $B_0 = 4(b+d)$ $\zeta = \sqrt{(n\rho)^2+2n\rho} - n\rho,\ n = \frac{E_s}{E_c} = \frac{2\times10^5}{4300\sqrt{f_c}}$
Elsanadedy et al. [84]	$V_n = 0.127\sqrt[3]{f_c}\sqrt{\rho f_y}\left(1+\frac{8d}{B_0}\right)\sqrt{1+\frac{125}{d}}B_0 d$ $B_0 = 4(b+d)$

when rapid decision-making or a large number of simulations are required. Moreover, FEM simulations often necessitate advanced technical expertise and specialised software, which may not always be readily available or accessible to engineers and practitioners.

On the other hand, the GPR model, as a ML method, offers several advantages in terms of time efficiency and practicality. Once the GPR model is trained with optimised hyperparameters, it can make rapid predictions with minimal computational resources, making it a more efficient and accessible tool for engineers and practitioners. Additionally, ML models can be implemented in various programming languages and environments, allowing for a broader range of applications and easier integration into existing workflows.

5.2. Developing a User-Friendly Application Interface. A user-friendly standalone application has been developed using the MATLAB Compiler, which is accessible on GitHub at the following link: https://github.com/lekhuong/PunchingSheaRCSlabs The tool combines the power of two powerful ML models, GPR and SVM; with the accuracy of three commonly used industry standards and three empirical equations from previous studies. The software is designed to be user-friendly, requiring the input of six variables with specified units of "MPa" for f_c and f_y, and "mm" for d, b, and a. Upon pressing the "calculate" button, the PSS of the slab is predicted in real time (Figure 12).

The user interface is designed with an intuitive layout, displaying input values in the upper left corner and predictive results in the upper right corner. The user can compare

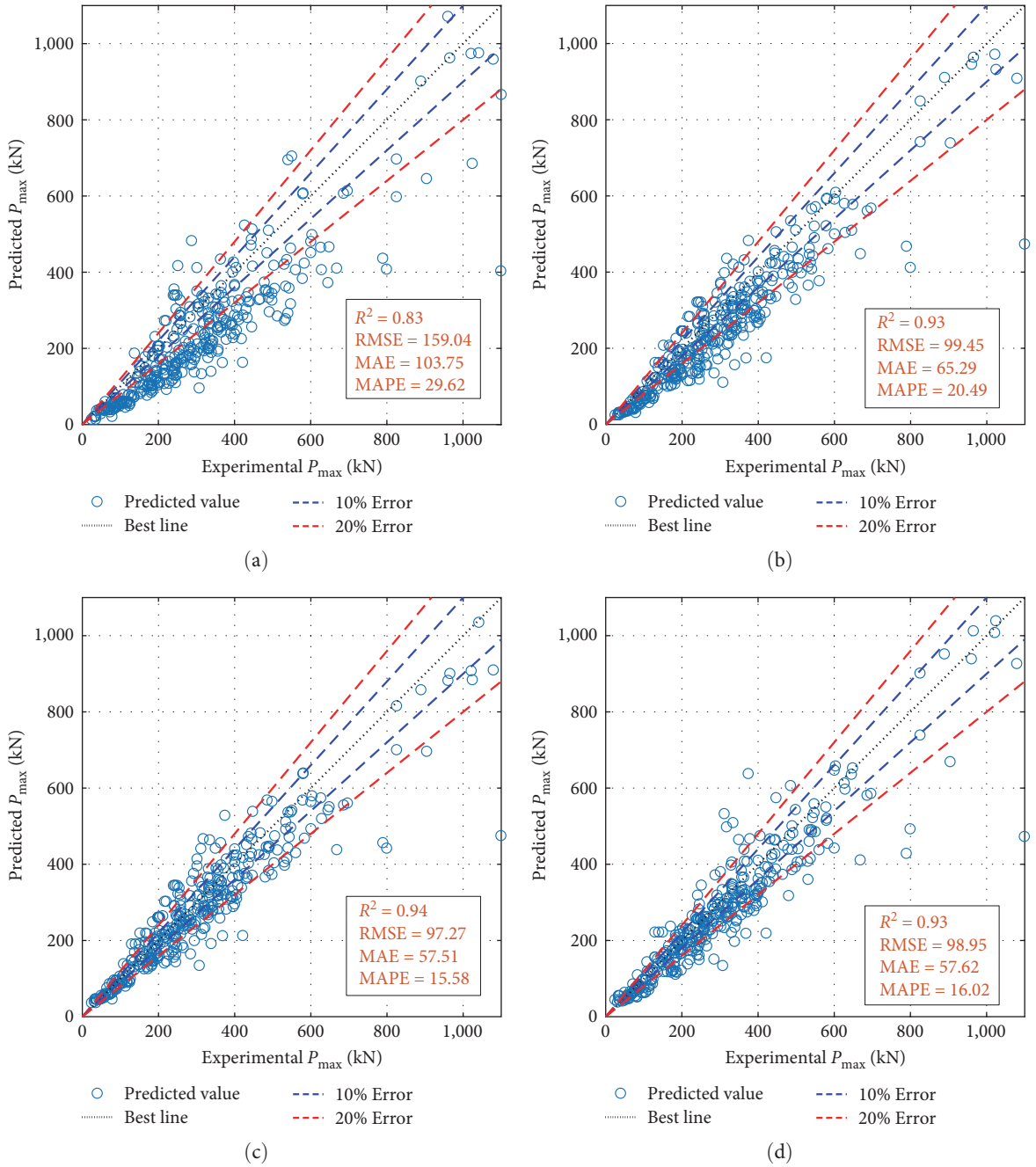

Figure 11: Continued.

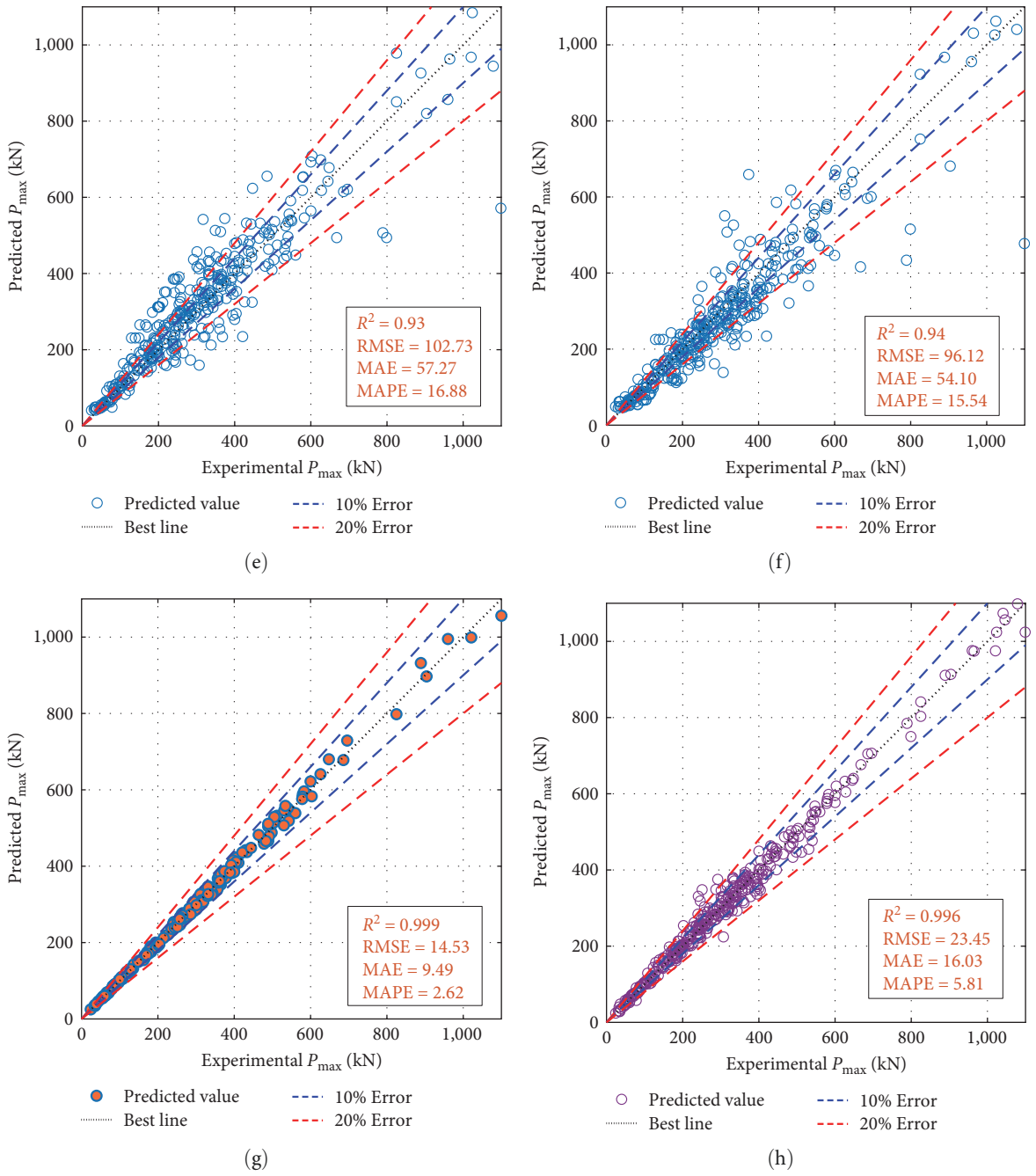

Figure 11: Prediction results of punching shear resistance per design codes, empirical, and developed models. (a) ACI 318-19; (b) EC2; (c) BS 8110-97; (d) Jabbar et al. [83]; (e) Chetchotisak et al. [7]; (f) Elsanadedy et al. [84]; (g) FEM simulations; and (h) GPR model.

Table 6: Statistical criteria values of design codes and empirical formulas in predicting the punching shear strength of flat slabs without transverse reinforcement.

Reference	Performance measurement				
	MAE	MSE	RMSE	R^2	MAPE
ACI 319-19 [80]	103.75	25,296	159.05	0.831	29.62
EC2 [81]	65.29	9,890	99.45	0.934	20.49
BS 8110-97 [82]	57.51	9,461	97.27	0.937	15.58
Jabbar et al. [83]	57.63	9,791	98.95	0.935	16.03
Chetchotisak et al. [7]	57.27	10,555	102.74	0.929	16.88
Elsanadedy et al. [84]	54.10	9,238	96.12	0.938	15.54
FEM simulations (227/379 predictions)	9.49	211	14.53	0.999	2.62
GPR model	16.03	549	23.45	0.996	5.81

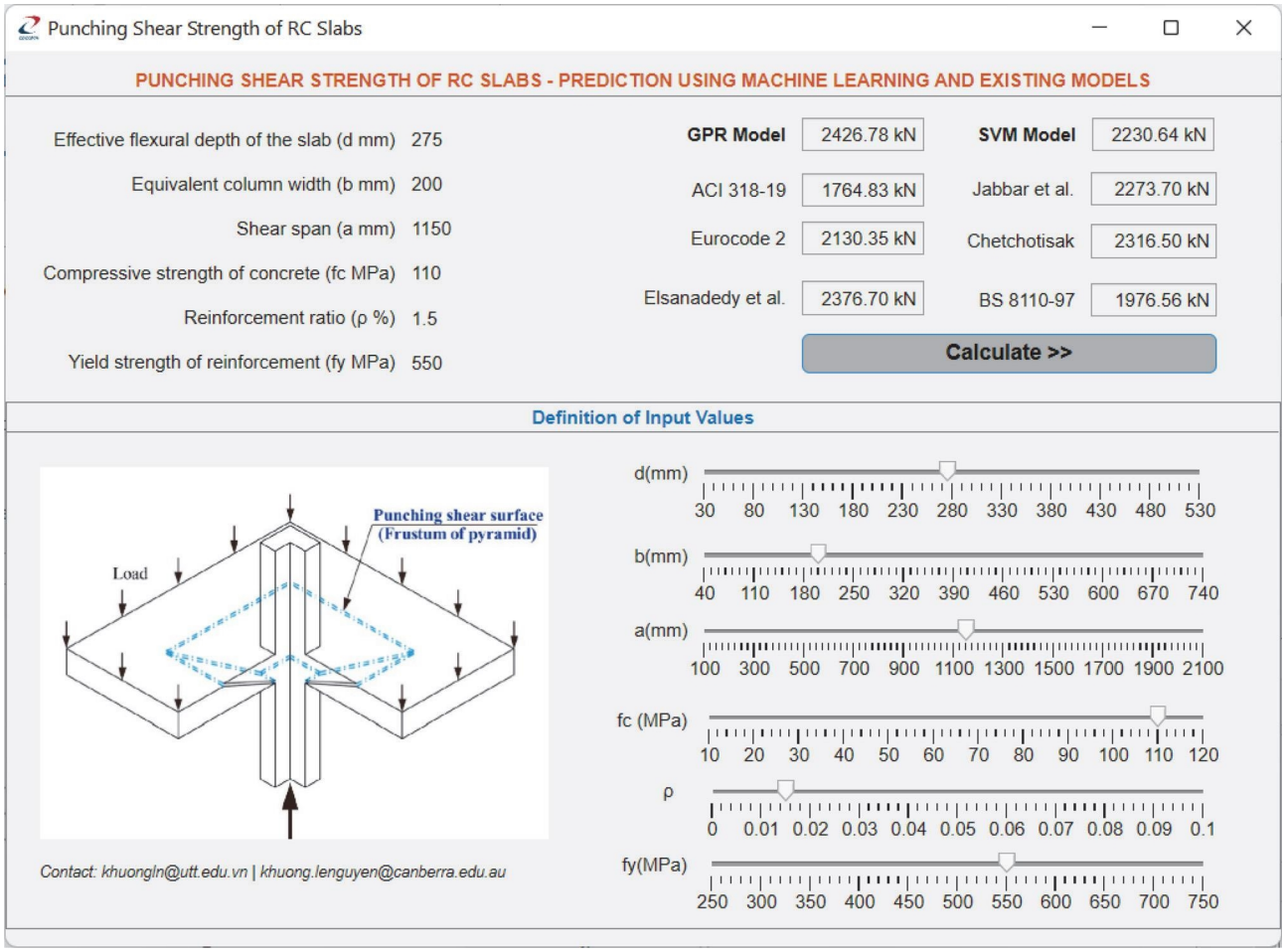

Figure 12: User-friendly standalone application.

the results of the GPR and SVM models with the calculated values based on practical standards such as ACI 318-19, Eurocode 2, and BS 8110-97, as well as the empirical equations created by Elsanadedy et al. [84], Jabbar et al. [83], and Chetchotisak et al. [7]. The tool offers the user the flexibility to choose the most appropriate model for their specific needs, providing reliable and accurate results for the PSS of RC slabs.

6. Conclusions

This research has successfully demonstrated the potential of ML models, specifically GPR and SVM, for predicting the PSS of RC slabs without transverse reinforcement. The study has also highlighted the advantages of low-code applications, such as MATLAB Regression Learner app, and MATLAB App Designer in streamlining the development of ML process

and facilitating the creation of user-friendly applications for engineering applications.

The research employed a comprehensive database of 379 RC slab samples and utilised both Random Search and Bayesian optimisation for hyperparameter tuning. The results indicated that even the default hyperparameters suggested by the Regression Learner app could yield satisfactory results, emphasising the benefits of using low-code tool, such as Regression Learner app, for rapid prototyping and efficient implementation.

FEM simulations were conducted using the nonlinear pushover technique and automated through MATLAB-Cast3M. Despite the limitations of nonconverged simulations, the FEM results exhibited exceptional performance, with the GPR model achieving the highest predictive accuracy among all models.

A total of 600 Monte Carlo simulations were performed to assess the robustness of the models, with the GPR model demonstrating superior predictive capability, achieving an R^2 value of around 0.99 for all databases. This result underscores the potential of GPR as a powerful tool for estimating the PSS of RC slabs in practical applications.

Finally, a user-friendly standalone application was developed using MATLAB's app Designer, offering real-time predictions of the PSS using the GPR and SVM models, as well as six empirical models from the literature. This application serves as a valuable resource for practitioners and researchers, allowing them to choose the most appropriate model for their specific needs and obtain reliable, accurate results for RC slab design.

Data Availability

All data will be available on request after the publication of this work.

Conflicts of Interest

The authors declare that they have no conflicts of interest.

References

[1] K. Qian and B. Li, "Load-resisting mechanism to mitigate progressive collapse of flat slab structures," *Magazine of Concrete Research*, vol. 67, no. 7, pp. 349–363, 2015.

[2] S. R. Vadyala, S. N. Betgeri, J. C. Matthews, and E. Matthews, "A review of physics-based machine learning in civil engineering," *Results in Engineering*, vol. 13, Article ID 100316, 2022.

[3] T. D. Akinosho, L. O. Oyedele, M. Bilal et al., "Deep learning in the construction industry: a review of present status and future innovations," *Journal of Building Engineering*, vol. 32, Article ID 101827, 2020.

[4] M. L. Castro Pena, A. Carballal, N. Rodríguez-Fernández, I. Santos, and J. Romero, "Artificial intelligence applied to conceptual design. A review of its use in architecture," *Automation in Construction*, vol. 124, Article ID 103550, 2021.

[5] C. Málaga-Chuquitaype, "Machine learning in structural design: an opinionated review," *Frontiers in Built Environment*, vol. 8, 2022.

[6] A. A. Elshafey, E. Rizk, H. Marzouk, and M. R. Haddara, "Prediction of punching shear strength of two-way slabs," *Engineering Structures*, vol. 33, no. 5, pp. 1742–1753, 2011.

[7] P. Chetchotisak, P. Ruengpim, D. Chetchotsak, and S. Yindeesuk, "Punching shear strengths of RC slab–column connections: prediction and reliability," *KSCE Journal of Civil Engineering*, vol. 22, no. 8, pp. 3066–3076, 2018.

[8] V.-L. Tran and S.-E. Kim, "A practical ANN model for predicting the PSS of two-way reinforced concrete slabs," *Engineering with Computers*, vol. 37, no. 3, pp. 2303–2327, 2021.

[9] H. D. Nguyen, G. T. Truong, and M. Shin, "Development of extreme gradient boosting model for prediction of punching shear resistance of r/c interior slabs," *Engineering Structures*, vol. 235, Article ID 112067, 2021.

[10] G. Doğan and M. H. Arslan, "Determination of punching shear capacity of concrete slabs reinforced with FRP bars using machine learning," *Arabian Journal for Science and Engineering*, vol. 47, no. 10, pp. 13111–13137, 2022.

[11] C. E. Rasmussen, "Gaussian processes in machine learning," in *Advanced Lectures on Machine Learning*, O. Bousquet, U. von Luxburg, and G. Rätsch, Eds., Springer, Berlin, Heidelberg, ML Summer Schools 2003, Canberra, Australia, February 2–14, 2003, 2003.

[12] J. Bergstra and Y. Bengio, "Random search for hyper-parameter optimization," *Journal of Machine Learning Research*, vol. 13, pp. 281–305, 2012.

[13] P. I. Frazier, "A tutorial on Bayesian optimization," 2018.

[14] K. Le Nguyen, H. Thi Trinh, T. T. Nguyen, and H. D. Nguyen, "Comparative study on the performance of different machine learning techniques to predict the shear strength of RC deep beams: model selection and industry implications," *Expert Systems with Applications*, vol. 230, Article ID 120649, 2023.

[15] A. H. Victoria and G. Maragatham, "Automatic tuning of hyperparameters using Bayesian optimisation," *Evolving Systems*, vol. 12, no. 1, pp. 217–223, 2021.

[16] K. Le-Nguyen, X.-H. Nguyen, H. C. Nguyen, M.-Q. Cao, A. Si Larbi, and Z. I. Djamai, "Experimental and numerical investigations of punching shear behavior of FRCM-strengthened two-way RC slabs," *Journal of Composites for Construction*, vol. 27, no. 1, Article ID 04022090, 2023.

[17] R. Z. Al-Rousan and B. R. Alnemrawi, "Punching shear code provisions examination against the creation of an opening in existed RC flat slab of various sizes and locations," *Structures*, vol. 49, pp. 875–888, 2023.

[18] R. Z. Alrousan and B. R. Alnemrawi, "The influence of concrete compressive strength on the punching shear capacity of reinforced concrete flat slabs under different opening configurations and loading conditions," *Structures*, vol. 44, pp. 101–119, 2022.

[19] R. Z. Alrousan and B. R. Alnemrawi, "Punching shear behavior of FRP reinforced concrete slabs under different opening configurations and loading conditions," *Case Studies in Construction Materials*, vol. 17, Article ID e01508, 2022.

[20] Y. Freund and R. E. Schapire, "A decision-theoretic generalization of on-line learning and an application to boosting," *Journal of Computer and System Sciences*, vol. 55, no. 1, pp. 119–139, 1997.

[21] C. Cortes and V. Vapnik, "Support-vector networks," *Machine Learning*, vol. 20, no. 3, pp. 273–297, 1995.

[22] C. Zhang and Y. Ma, *Ensemble Machine Learning: Methods and Applications*, Springer, April 2012.

[23] E. Le Fichoux, "Présentation Et Utilisation De Cast3m," 2011, http://www-cast3m.cea.fr/.

[24] J. Mazars, "A description of micro- and macroscale damage of concrete structures," *Engineering Fracture Mechanics*, vol. 25, no. 5-6, pp. 729–737, 1986.

[25] J. Mazars, F. Hamon, and S. Grange, "A new 3D damage model for concrete under monotonic, cyclic and dynamic loadings," *Materials and Structures*, vol. 48, no. 11, pp. 3779–3793, 2015.

[26] J. Browning, S. Pujol, R. Eigenmann, and J. A. Ramirez, "NEEShub databases," *Concrete International*, vol. 35, pp. 55–60, 2013.

[27] S. Ozden, U. Ersoy, and T. Ozturan, "Punching shear tests of normal-and high-strength concrete flat plates," *Canadian Journal of Civil Engineering*, vol. 33, no. 11, pp. 1389–1400, 2006.

[28] S. Guandalini, "*Poinçonnement symétrique des dalles*," Ph.D. thesis, École Polytechnique Féderale de Lausanne, Switzerland, 2005.

[29] G. Birkle, "*Punching of flat slabs: the influence of slab thickness and stud layout*," Ph.D. Thesis, Birkle G, Canada, 2004.

[30] M. Timm, "*Durchstanzen von Bodenplatten unter rotationssymmetrischer Belastung*," Ph.D. Thesis, Deutscher Ausschuss Für Stahlbeton, Berlin, 2004.

[31] D. R. C. Oliveira, P. E. Regan, and G. S. S. A. Melo, "Punching resistance of RC slabs with rectangular columns," *Magazine of Concrete Research*, vol. 56, no. 3, pp. 123–138, 2004.

[32] C. E. Ospina, S. D. Alexander, and J. R. Cheng, "Punching of two-way concrete slabs with fiber-reinforced polymer reinforcing bars or grids," *Structural Journal*, vol. 100, pp. 589–598, 2003.

[33] K. K. L. Li, *Influence of Slab Thickness on Punching Shear Strength*, McGill University, Canada, 2000.

[34] S. Matthys and L. Taerwe, "Concrete slabs reinforced with FRP grids. II: punching resistance," *Journal of Composites for Construction*, vol. 4, pp. 154–161, 2000.

[35] P. J. McHarg, W. D. Cook, D. Mitchell, and Y. S. Yoon, "Benefits of concentrated slab reinforcement and steel fibers on performance of slab–column connections," *ACI Structural Journal*, vol. 97, pp. 225–234, 2000.

[36] M. Ozawa, Y. Uchida, and W. Koyanagi, "Study on the process on punching shear failure of RC slabs," in *International Workshop on Punching Shear Capacity of RC Slabs*, pp. 145–154, Royal Institute of Technology, Stockholm, Sweden, 2000.

[37] C. M. Ghannoum, "Effect of high-strength concrete on the performance of slab–column specimens," *ACI Structural Journal*, vol. 95, no. 3, Article ID 227, 1998.

[38] E. Sistonen, M. Lydman, and S. Huovinen, *Asuinrakennusten välipohjalaattojen raudoitustapojen teknis-taloudellinen vertailu, Julkaisu/Report No.69*, Talonrakennustekniikka, Teknillinen Korkeakoulu, Espoo, Finland, 1997.

[39] M. Hallgren, "*Punching shear capacity of reinforced high strength concrete slabs*," Ph.D. Thesis, Royal Institute of Technology, Stockholm, Sweden, 1996.

[40] K. E. M. Ramdane, "Punching shear of high performance concrete slabs," in *4th International Symposium on Utilization of High-Strength/High Performance Concrete*, vol. 3, pp. 1015–1026, 1996.

[41] N. Banthia, M. Al-Asaly, and S. Ma, "Behavior of concrete slabs reinforced with fiber-reinforced plastic grid," *Journal of Materials in Civil Engineering*, vol. 7, no. 4, pp. 252–257, 1995.

[42] T. Urban, "Nośność na przebicie w aspekcie proporcji boków słupa, Wydawn," in *Katedry Budownictwa Betonowego Wydziału Budownictwa, Architektury i Inżynierii Środowiska Politechniki Łódzkiej*, 1994.

[43] D. D. Theodorakopoulos and N. Swamy, "Contribution of steel fibers to the strength characteristics of lightweight concrete slab–column connections failing in punching shear," *Structural Journal*, vol. 90, pp. 342–355, 1993.

[44] A. Tomaszewicz, "High strength concrete: SP2—plates and shells report 2.3," in *Punching shear capacity of reinforced concrete slabs, Report No. STF70-A93082*, SINTEF (Selskapet for Industriell Og Teknisk Forskning, Trondgeim), Norway, 1993.

[45] S. D. Alexander and S. H. Simmonds, "Tests of column-flat plate connections," *Structural Journal*, vol. 89, pp. 495–502, 1992.

[46] H. Marzouk and A. Hussein, "Experimental investigation on the behavior of high-strength concrete slabs," *Structural Journal*, vol. 88, pp. 701–713, 1992.

[47] N. J. Gardner, "Relationship of the punching shear capacity of reinforced concrete slabs with concrete strength," *Structural Journal*, vol. 87, pp. 66–71, 1990.

[48] J. S. Lovrovich and D. I. McLean, "Punching shear behavior of slabs with varying span-depth ratios," *Structural Journal*, vol. 87, pp. 507–512, 1990.

[49] P. Tolf, *Influence of the Slab Thickness on the Strength of Concrete Slabs at Punching: Tests with Circular Slabs No. 146*, Royal Institute of Technology, Stockholm, Sweden, 1998.

[50] G. I. B. Rankin and A. E. Long, "Predicting the punching strength of conventional slab–column specimens," *Proceedings of the Institution of Civil Engineers*, vol. 82, no. 2, pp. 327–346, 1987.

[51] P. E. Regan, "Symmetric punching of reinforced concrete slabs," *Magazine of Concrete Research*, vol. 38, no. 136, pp. 115–128, 1986.

[52] Menétrey, "The dependence of punching resistance upon the geometry of the failure surface," *Magazine of Concrete Research*, vol. 36, no. 126, pp. 3–8, 1994.

[53] U. Schaefers, *Bemessung und Sicherheit gegen Durchstanzen von balkenlosen Stahlbetondecken im Bereich der Innenstützen*, Deutscher Ausschuss für Stahlbeton, 1984.

[54] R. N. Swamy and S. A. R. Ali, "Punching shear behavior of reinforced slab–column connections made with steel fiber concrete," *Journal Proceedings*, vol. 79, no. 5, pp. 392–406, 1982.

[55] J. Pralong, W. Brändli, and B. Thürlimann, *Durchstanzversuche an stahlbeton-und spannbetonplatten*, Birkhäuser, 1979.

[56] M. Ladner, W. Schaeidt, and S. Gut, "Experimentelle untersuchungen an Stahlbeton-Flachdecken," in *Bericht Nr.205*, EMPA, Dübendorf, Swiss, 1977.

[57] J. Pralong, B. Thürlimann, and P. Marti, "Schubversuche an Stahlbeton-Platten, Bericht/Institut Für Baustatik Und Konstruktion ETH Zürich. 7305," 1977.

[58] M. E. Criswell, "Static and dynamic response of reinforced concrete slab–column connections," *Special Publication*, vol. 42, pp. 721–746, 1974.

[59] A. E. Long and D. M. Masterson, "Improved experimental procedure for determining the punching strength of reinforced concrete flat slab structures," *Special Publication*, vol. 42, pp. 921–938, 1974.

[60] M. Ladner, "Einfluß der Maßstabgröße bei Durchstanzversuchen," *Material Und Technik*, vol. 1, pp. 60–68, 1973.

[61] H. Nylander and H. Sundquist, "Genomstansning av pelarunderstödd plattbro av betong med ospänd armering,"

in *Nr 104. Stockholm*, Institutionen för byggnadsstatik, Kungl Tekniska högskolan, Stockholm, Sweden, 1972.
[62] N. M. Hawkins, H. B. Fallsen, and R. C. Hinojosa, "Influence of column rectangularity on the behavior of flat plate structures," *Special Publication*, vol. 30, pp. 127–146, 1971.
[63] F. Roll, S. T. H. Zaidi, G. Sabnis, and G. Sabnis, "Shear resistance of perforated reinforced concrete slabs," *ACI Special Publication*, vol. 30, pp. 77–102, 1971.
[64] Ladner M. Beutel and A. Rösli, *Berechnung von Flachdecken auf Durchstanzen, Edigenössische Materialprüfugs*, Und Versuchsanstalt, Dübendorf, 1970.
[65] W. G. Corley and N. M. Hawkins, "Shear head reinforcement of slabs," *Journal Proceedings*, vol. 65, no. 10, pp. 811–824, 1968.
[66] R. D. Mowrer and M. D. Vanderbilt, "Shear strength of lightweight aggregate reinforced concrete flat plates," *Journal Proceedings*, pp. 722–729, 1967.
[67] S. Kinnunen, *Punching of Structural Concrete Slabs: Technical Report*, fib Fédération internationale du béton, 2001.
[68] M. J. Manterola, "Behavior of beams and punching in slabs without shear reinforcement, in: Comité Euro-International du Béton," *Bulletin d'Information*, vol. 62, 1966.
[69] D. Yitzhaki, "Punching strength of reinforced concrete slabs," *Journal Proceedings*, vol. 63, no. 5, pp. 527–542, 1966.
[70] R. Taylor and B. Hayes, "Some tests on the effect of edge restraint on punching shear in reinforced concrete slabs," *Magazine of Concrete Research*, vol. 17, no. 50, pp. 39–44, 1965.
[71] J. Moe, *Shearing Strength of Reinforced Concrete Slabs and Footings under Concentrated Loads*, Portland Cement Association, 4th edition, 1961.
[72] S. A. Kinnunen and H. Nylander, "Punching of concrete slabs without shear reinforcement," in *Royal Institute of Technology, Transactions, No. 158*, Stockholm, Sweden, 1960.
[73] G. D. Base, "Some tests on the punching shear strength of reinforced concrete slabs," Technical Report No. 321Cement and Concrete Association, 1959.
[74] I. J. W. Rosenthal, "Experimental investigation of flat plate floors," *Journal Proceedings*, vol. 56, no. 8, pp. 153–166, 1959.
[75] R. C. Elstner and E. Hognestad, "Shearing strength of reinforced concrete slabs," *Journal Proceedings*, pp. 29–58, 1956.
[76] C. Forssell, E. Holmberg, and E., "Concentrated loads on concrete slabs," *Betong*, vol. 31, no. 2, pp. 95–123, 1946.
[77] F. E. Richart and R. W. Kluge, *Tests of Reinforced Concrete Slabs Subjected to Concentrated Loads: A Report of an Investigation*, Bulletin Series No.314, University of Illinois Urbana, Illinois, 1939.
[78] O. Graf, "Versuche über die Widerstandsfähigkeit von allseitig aufliegenden dicken Eisenbetonplatten unter Einzellasten," vol. Heft 88, Deutscher Ausschuß Für Eisenbeton, Berlin, Germany, 1938.
[79] M. Papadrakakis and N. D. Lagaros, "Reliability-based structural optimisation using neural networks and Monte Carlo simulation," *Computer Methods in Applied Mechanics and Engineering*, vol. 191, no. 32, pp. 3491–3507, 2002.
[80] ACI Committee 318, *Building Code Requirements for Structural Concrete (ACI 318- 19) and Commentar*, American Concrete Institute, Farmington Hills, MI, 2019.
[81] P. Code, *Eurocode 8: Design of Structures for Earthquake Resistance-Part 1: General Rules, Seismic Actions and Rules for Buildings*, European Committee for Standardization, Brussels, 2005.
[82] BSI, "BS 8110, Structural use of concrete—part 1: code of practice for design and construction," 1997.
[83] A. S. A. Jabbar, M. A. Alam, and K. N. Mustapha, "A new equation for predicting punching shear strength of R/C flat plates," in *Proceedings National Graduate Conference*, 2012.
[84] H. M. Elsanadedy, Y. A. Al-Salloum, and S. H. Alsayed, "Prediction of punching shear strength of HSC interior slab–column connections," *KSCE Journal of Civil Engineering*, vol. 17, no. 2, pp. 473–485, 2013.